

1 *Published as: Cusack, P.B., Callery, O., Courtney, R., Ujaczki, E., O' Donoghue, L.M.T.,*  
2 *Healy, M.G. 2019. The use of rapid small-scale column tests to determine the efficiency of*  
3 *bauxite residue as a low-cost adsorbent in the removal of dissolved reactive phosphorus.*  
4 *Journal of Environmental Management 241: 273-283.*  
5 *doi.org/10.1016/j.jenvman.2019.04.042*  
6

7 The use of rapid, small-scale column tests to determine the efficiency of bauxite residue as a  
8 low-cost adsorbent in the removal of dissolved reactive phosphorus from agricultural waters.

9

10 Patricia B. Cusack<sup>a,b,c</sup>, Oisín Callery<sup>d</sup>, Ronan Courtney<sup>a,c</sup>, Éva Ujaczki<sup>c,e,f</sup> Lisa M. T. O'  
11 Donoghue<sup>f</sup>, Mark G. Healy<sup>b\*</sup>

12

13 <sup>a</sup>Department of Biological Sciences, University of Limerick, Castletroy, Co. Limerick,  
14 Ireland.

15 <sup>b</sup>Civil Engineering, National University of Ireland, Galway, Ireland.

16 <sup>c</sup>The Bernal Institute, University of Limerick, Castletroy, Co. Limerick, Ireland.

17 <sup>d</sup>Earth and Ocean Sciences, National University of Ireland, Galway, Ireland.

18 <sup>e</sup>Department of Applied Biotechnology and Food Science, Faculty of Chemical Technology  
19 and Biotechnology, Budapest University of Technology and Economics, Műegyetem rkp. 3,  
20 1111 Budapest, Hungary.

21 <sup>f</sup>School of Engineering, University of Limerick, Castletroy, Co. Limerick, Ireland.

22

23 \*Corresponding Author. Tel: +353 91 495364; fax: +353 91 494507. Postal address: Alice  
24 Perry Engineering Building, College of Engineering and Informatics, National University of  
25 Ireland, Galway, Co. Galway, H91 HX31. E-mail address: [mark.healy@nuigalway.ie](mailto:mark.healy@nuigalway.ie)

26

## 27 **Highlights**

28 • Bauxite residue was examined as an adsorbent for phosphorus using a column study.

- 29       • The bauxite residue had a service time of 1.08 min g<sup>-1</sup> media for the forest run-off.  
30       • The service time was 0.28 min g<sup>-1</sup> media when treating dairy soiled water.  
31       • The bauxite residue was examined before and after the adsorption process.

32

### 33 **Abstract**

34

35 Bauxite residue, the by-product produced in the alumina industry, is a potential low-cost  
36 adsorbent in the removal of phosphorus (P) from aqueous solution, due to its high  
37 composition of residual iron oxides such as hematite. Several studies have investigated the  
38 performance of bauxite residue in removing P; however, the majority have involved the use  
39 of laboratory “batch” tests, which may not accurately estimate its actual performance in filter  
40 systems. This study investigated the use of rapid small-scale column tests to predict the  
41 dissolved reactive phosphorus (DRP) removal capacity of bauxite residue when treating two  
42 agricultural waters of low (forest run-off) and high (dairy soiled water) phosphorus content.  
43 Bauxite residue was successful in the removal of DRP from both waters, but was more  
44 efficient in treating the forest run-off. The estimated service time of the column media, based  
45 on the largest column studied, was 1.08 min g<sup>-1</sup> media for the forest run-off and 0.28 min g<sup>-1</sup>  
46 media for the dairy soiled water, before initial breakthrough time, which was taken to be  
47 when the column effluent reached approximately 5% of the influent concentration, occurred.  
48 Metal(loid) leaching from the bauxite residue, examined using ICP-OES, indicated that  
49 aluminium and iron were the dominant metals present in the treated effluent, both of which  
50 were above the EPA parametric values (0.2 mg L<sup>-1</sup> for both Al and Fe) for drinking water.

51

52 **Keywords:** bauxite residue; adsorbent; phosphorus; agricultural wastewater

53

54 **Nomenclature**

55

56 A constant of proportionality ( $\text{mg g}^{-1}$ )

57  $a^{**}$  a time constant.

58 Al aluminium

59  $\text{Al}_2\text{O}_3$  aluminium oxide

60 As arsenic

61 B constant of system heterogeneity in Eqn. (1 and 2)

62 BRDA bauxite residue disposal area

63 Ca calcium

64 Cd cadmium

65  $C_t$  solution adsorbate concentration at any filter depth ( $\text{mg L}^{-1}$ )

66  $C_o$  influent contaminant concentration ( $\text{mg L}^{-1}$ )

67 Cr chromium

68 CRM critical raw material

69 Cu copper

70 DRP dissolved reactive phosphorus ( $\text{mg L}^{-1}$ )

71 DSW dairy soiled water

72 EDS energy-dispersive X-ray spectroscopy

73 Fe iron

74  $\text{Fe}_2\text{O}_3$  iron oxide

75 F1 fluoride

76 FT-IR Fourier transform infrared

77 Ga gallium

78 Hg mercury

79	HNO <sub>3</sub>	nitric acid
80	ICP-OES	inductively coupled plasma optical emission spectrometer
81	M	mass of filter media contained in the filter column (g)
82	Mg	magnesium
83	Mn	manganese
84	Mo	molybdenum
85	n	the number of containers in which the total volume of effluent is collected
86	N	nitrogen
87	Na	sodium
88	Ni	nickel
89	P	phosphorus
90	Pb	lead
91	pH	pH unit
92	q <sub>e</sub>	cumulative mass of contaminant adsorbed per g of filter media (mg g <sup>-1</sup> )
93	q <sub>t</sub>	time dependent sorbate concentration per unit mass of adsorbent (mg g <sup>-1</sup> ),
94	RSSCT	rapid small-scale column test
95	Se	selenium
96	SEM	scanning electron microscopy
97	t	Empty bed contact time of the column filter bed (min)
98	V	volume of the influent loaded onto the filter (L)
99	V	vanadium
100	V <sub>B</sub>	number of empty bed volumes of influent/solution filtered
101	XRD	x-ray diffraction
102	XRF	x-ray fluorescence
103	Zn	zinc

## 104 **1. Introduction**

105

106 Phosphorus (P) is an essential component of all plant and animal life (Weissert and Kehr,  
107 2018), and is critical in the production and maintenance of food supply (Cordell and White  
108 2011; Pretty and Bharucha, 2014). Phosphorus is also identified as one of the key nutrients  
109 that leads to the eutrophication of water bodies, in which there is an excess production of  
110 algal blooms, resulting in detrimental effects to aquatic life (Pan *et al.*, 2018). Agricultural  
111 practices, such as the application of slurry and fertiliser, may result in the transport of  
112 nutrients in surface runoff (Murnane *et al.*, 2016; Pan *et al.*, 2018) and subsurface flow (O'  
113 Flynn *et al.*, 2018; Zhou *et al.*, 2016) to a water body, and have been identified as a major  
114 cause of eutrophication (Sharpley, 2016).

115

116 The movement of P from soil to water bodies is predominantly in the form of particulate or  
117 dissolved reactive P (DRP) (Brennan *et al.*, 2014), the latter being 100% available for aquatic  
118 biota and which, therefore, has an immediate effect on the surrounding ecosystems (Penn *et*  
119 *al.*, 2014). Conventional methods of P removal from water have involved the use of  
120 enhanced biological removal systems such as polyphosphate accumulating organisms (PAOs)  
121 (Ge *et al.*, 2015) and algal biofilms (Sukačová *et al.*, 2015), precipitation methods using  
122 hydrous ferric oxides (Hauduc *et al.*, 2015) or struvite (Zhou *et al.*, 2015), the use of  
123 adsorbents (Grace *et al.*, 2015; Callery *et al.*, 2016; Callery and Healy, 2017), ion exchange  
124 (Acelas *et al.*, 2015), and reverse osmosis (Wang *et al.*, 2016). In recent years, to address the  
125 concept of a 'circular economy' (United Nations, 2015), emphasis has been placed on the  
126 utilisation of industrial wastes as low-cost adsorbents (De Gisi *et al.*, 2016; Grace *et al.*,  
127 2016). Materials that have been utilised include fly ash (Nowak *et al.*, 2013), steel slags  
128 (Claveau-Mallet *et al.*, 2013) and chemical amendments (Callery *et al.*, 2015). Particular

129 focus has been placed on bauxite residue (red mud), the by-product generated in the Bayer  
130 Process during the extraction of alumina, as a potential low-cost P adsorbent in aqueous  
131 solutions. It is currently being produced at a global rate of 150 Mt per annum (Evans 2016),  
132 but only approximately 2 % of the bauxite residue produced is currently re-used (Ujaczki *et*  
133 *al.*, 2018), with the remaining ~ 98% being disposed of into bauxite residue disposal areas  
134 (BRDAs) (Burke *et al.*, 2013; Kong *et al.*, 2017). The general composition of bauxite residue  
135 comprises high amounts of iron (Fe) and aluminium (Al) oxides (Zhu *et al.*, 2016), which are  
136 good adsorbents of P. In addition, bauxite residue has a high specific surface area (Gräfe *et*  
137 *al.*, 2011) and therefore has numerous potential adsorption sites, giving it increased capacity  
138 for P retention. Previous laboratory studies have shown that bauxite residue has high P  
139 adsorption capacity (Table 1).

140

141 Traditionally, bench-scale “batch” studies are conducted to evaluate the effectiveness of a  
142 material to adsorb P (Table 1). These studies involve placing the material in small containers,  
143 overlaying it with solutions of known concentrations, mixing for a period usually of between  
144 24 to 48 hr, and then fitting the results obtained to an adsorption isotherm such as the  
145 Freundlich or Langmuir, in order to quantify its adsorption potential (Cusack *et al.*, 2018;  
146 Grace *et al.*, 2015). However, batch studies have some disadvantages, such as failing to  
147 replicate the often passive nature of the adsorption process which exists on site, as well as  
148 sometimes using unrealistic ratios of adsorbent to solution, and shaking of the samples  
149 (ÁdÁm *et al.*, 2007; Søvik and Kløve, 2005). In addition, concerns have been raised about  
150 their accuracy in replicating the actual performance when the adsorbent material is placed in  
151 a filter and operated on site (Fenton *et al.*, 2009). Due to the nature of the batch experiment,  
152 they also fail to realistically replicate any incidental releases of contaminants, which may  
153 occur when some materials are placed in filters. This may be particularly pertinent in the

154 evaluation of the feasibility of bauxite residue, which contains metals (Cusack *et al.*, 2018).  
155 In order to determine the full potential and longevity of an adsorbent, larger scale “column”  
156 studies are necessary (Pratt *et al.*, 2012). In these studies, the material is placed in a column,  
157 usually operated at laboratory-scale, and water of a known concentration is passed through  
158 the material until the effluent concentration is the same as the influent concentration. These  
159 continuous flow column studies require vast amounts of influent water, which depending on  
160 the type of water utilised, is often difficult to source in the laboratory (Callery and Healy,  
161 2017). On account of this, rapid, small-scale column studies which utilise smaller volumes of  
162 media and wastewater have been gaining in popularity, and have been used to successfully  
163 model the adsorbancies of P (Callery *et al.*, 2016; Lalley *et al.*, 2015), fluoride (Wu *et al.*,  
164 2018), paracetamol (García-Mateos *et al.*, 2015), and varying species of arsenic (Tresintsi *et*  
165 *al.*, 2014).

166

167 As P adsorption tests on bauxite residues have been commonly conducted using batch-scale  
168 studies, which may have many shortcomings as detailed above, the objectives of this study  
169 were to use rapid, small-scale column studies to (1) to assess the potential of bauxite residue  
170 as a low-cost adsorbent for DRP removal from two types of agricultural waters (dairy soiled  
171 water (DSW) and forest run-off) (2) compare the composition of the bauxite residue before  
172 and after use in the column tests (3) investigate the speciation of P adsorption onto the  
173 bauxite residue, and (4) identify any potential trace metal mobilisation from the bauxite  
174 residue during the study.

175

176

177

178

179 **2. Materials and Methods**

180 2.1 Sample collection

181 Bauxite residue was obtained from a European refinery. Residue was sampled to a depth of  
182 30 cm below the surface of the BRDA, returned to the laboratory and dried at 105 °C for 24  
183 hr. Once dry, the samples were pulverised using a mortar and pestle and sieved to a particle  
184 size < 0.5 mm. The pH and electrical conductivity (EC) were measured (n=3) using 5 g of  
185 sample in an aqueous extract, using a 1:5 ratio (solid:liquid) (Courtney and Harrington,  
186 2010). Dairy soiled water (milk parlour washings composed of cow faeces and urine, milk  
187 and detergents; Minogue *et al.*, 2015) was collected from Teagasc Agricultural Research  
188 Centre, Moorepark, Co. Cork, Ireland [52° 9' 48.114" N, 8° 15' 34.6464" W] and forest run-  
189 off was collected from Kilmoon, Co. Clare, Ireland [53° 2' 48.0372" N, 9° 16' 21.1368" W].  
190 The DSW and forest run-off were transferred directly to a temperature-controlled room  
191 (11 °C) prior to commencement of testing. The DRP was measured using filtered (0.45 µm)  
192 subsamples using a nutrient analyser (Konelab20, Thermo Clinical Lab systems, Finland) and  
193 the pH was measured using a Eutech Instruments pH 700 (Thermo Scientific, USA).

194

195 2.1.1 Media characterisation

196 The bauxite residue was characterised before and after the experiment. Mineralogical  
197 detection was carried out on 1 g powdered samples using X-ray diffraction (XRD) on a  
198 Philips X'Pert PRO MPD® (California, USA) at 40 kV, 40 mA, 25 °C by Cu X-ray tube (K $\alpha$ -  
199 radiation). The patterns were collected in the angular range from 5 to 80 ° (2 $\theta$ ) with a step-  
200 size of 0.008 ° (2 $\theta$ ) (Castaldi *et al.*, 2011). The surface morphology and elemental detection  
201 were carried out using scanning electron microscopy (SEM) and energy-dispersive X-ray  
202 spectroscopy (EDS) on a Hitachi SU-70 (Berkshire, UK). X-ray fluorescence (XRF) analysis  
203 was carried out onsite at the refinery using a Panalytical Axios XRF.

## 204 2.2 Rapid Small Scale Column Study

205 Small bore adsorption columns were prepared after Callery *et al.* (2016) using polycarbonate  
206 tubes, with an internal diameter of 0.94 cm and lengths of 20, 30 and 40 cm. The tubes were  
207 packed with a mixture of bauxite residue. The bauxite residue was held in place within each  
208 column using acid-washed glass wool and plastic syringes with an internal diameter equal to  
209 outside diameter of the polycarbonate tube, placed at the top and bottom of each of the  
210 polycarbonate tube columns. To each end of the polycarbonate tube column, flexible silicone  
211 tubing was attached to the syringe ends in order to provide lines for the influent and effluent.  
212 The columns were secured on a metal frame, allowing for a stable, vertical orientation to be  
213 maintained. A Masterflex® L/S Variable-Speed Drive peristaltic pump (Gelsenkirchen,  
214 Germany) with a variable speed motor was used to pump the influent, DSW and forest run-  
215 off, into the base of each column at an estimated flow rate of  $30.49 \pm 0.85 \text{ mL hr}^{-1}$  (equivalent  
216 to a hydraulic loading rate used in a P removal system for wastewater treatment on a poultry  
217 farm; Penn *et al.*, 2014). The pump was operated in 12 hr on/off cycles (to allow the filter  
218 media to replenish some of its adsorption sites) to achieve loading periods of 24 – 36 hr, in  
219 order to obtain enough data points for the determination of the adsorption model coefficients.  
220 Every 2 hr, aliquots of the filtered effluent were collected using an auto-sampler and  
221 measured for volume, pH and DRP.

222

223 The adsorption performance of the media was evaluated using a model developed by Callery  
224 and Healy (2017), wherein the column effluent ( $C_e$ ) is taken as a function of the volume of  
225 influent treated ( $V$ ) and breakthrough concentrations (BTCs) formed by plotting  $V$  (x-axis)  
226 against  $C_e$  (y-axis). The breakthrough of the column media was taken to be when the column  
227 effluent was approximately 5% of the influent concentration (Chen *et al.*, 2003). This model,  
228 which has been successful in the prediction of the performance of a large-scale filter (Callery

229 *et al.*, 2016), was used in the prediction of the longevity of the bauxite residue in the current  
230 study.

231

232 The overall bauxite residue service time or longevity of the bauxite residue media can be  
233 found by first determining the volume treated, using Eqn. 1, where  $q_t$  is the time dependent  
234 sorbate concentration per unit mass of adsorbent ( $\text{mg g}^{-1}$ ),  $M$  is the mass of the adsorbent (g),  
235  $B$  is a constant of system heterogeneity,  $C_o$  is the sorbate concentration of the influent ( $\text{mg L}^{-1}$ )  
236 and  $C_t$  is the solution adsorbate concentration at any filter depth ( $\text{mg L}^{-1}$ ), by dividing the  
237 volume treated,  $V$  (in L) by the loading rate ( $\text{L s}^{-1}$ ) and then converting to minutes per g of  
238 media.

239

240

$$V = \frac{q_t M}{B (C_o - C_t)}$$

241

(1)

242 The  $q_t$  used in Eqn. 1 was calculated using Eqn. 2:

243

244

$$q_t = AV_B \left( \frac{1}{B} \right) \left| \frac{t}{t+a^{**}} \right| \quad (2)$$

245

246 Where  $A$  is a constant of proportionality ( $\text{mg L}^{-1}$ ),  $t$  is the empty bed contact time of the  
247 column filter bed (min),  $V_B$  is the number of empty bed volumes of influent/solution filtered,  
248 and  $a^{**}$  is a time constant.

249

### 250 2.3 Speciation of P adsorbed

251 Fourier transform infrared (FT-IR) analysis was carried out using a Perkin Elmer Spectrum  
252 100 (PerkinElmer, USA). The FT-IR spectra were recorded in the  $4000$  to  $650 \text{ cm}^{-1}$  range  
253 and were collected after 256 scans at  $4 \text{ cm}^{-1}$  resolution (Castaldi *et al.*, 2010).

254

## 255 2.4 Trace metal analysis

256 Every 2 hr, 10 mL of the aliquot collected from the columns, was preserved in nitric acid  
257 (HNO<sub>3</sub>), to a pH <2 and refrigerated before elemental analysis was carried out using an  
258 Agilent Technologies 5100 Inductively Coupled Plasma Optical Emission Spectrometer (ICP-  
259 OES). In order to carry out the ICP-OES analysis, a calibration curve was created using  
260 standardised solutions comprised of 100, 50, 10, 5 and 1 g L<sup>-1</sup> multi element standard  
261 (Inorganic Ventures, Ireland) and 1M HNO<sub>3</sub>. The analytical lines (in nm) used for the  
262 calculations of each element were as follows: Al 237.312, 396.152; calcium (Ca) 396.847,  
263 422.673; cadmium (Cd) 214.439, 226.502, 228.802; chromium (Cr) 205.560, 267.716,  
264 357.868; copper (Cu) 213.598, 324.754, 327.395; Fe 234.350, 238.204, 259.940; gallium  
265 (Ga) 287.423, 294.363, 417.204; mercury (Hg) 184.887, 194.164; magnesium (Mg) 279.553,  
266 280.270, 285.213; manganese (Mn) 257.610, 259.372, 260.568; molybdenum (Mo) 202.032,  
267 203.846, 204.598; sodium (Na) 589.592; nickel (Ni) 216.555, 221.648, 231.604; lead (Pb)  
268 220.353, 283.305; selenium (Se) 196.026, 203.985; silicon (Si) 250.690, 251.611, 288.158;  
269 vanadium (V) 268.796, 292.401, 309.310; zinc (Zn) 202.548, 206.200, 213.857 (Bridger and  
270 Knowles, 2010). The XRF analysis performed on the bauxite residue was carried out using a  
271 Panalytical Axios XRF (Malvern Panalytical Ltd., United Kingdom).

272

## 273 **3. Results and Discussion**

### 274 3.1 Media characterisation before and after the experiments

275 Bauxite residue typically comprises Fe, Al, Ti, Si, Na and Ca, mainly in the form of oxides  
276 (Gräfe *et al.*, 2011). The presence of Fe and Al oxides, which can range from 5 to 60 and 5  
277 to 30 %, respectively (Evans, 2016), and Ti oxides, which are typically in the range of 0.3 to  
278 15 % (Evans, 2016), mean that bauxite residue is a potential adsorbent for both cations and

279 anions from aqueous solutions (Bhatnagar *et al.*, 2011; Cusack *et al.*, 2018). This is why  
280 numerous studies have investigated the potential of P removal from aqueous solution (Table  
281 1).

282

283 The main mineralogical composition of the bauxite residue used in this study comprised  
284 mainly iron and aluminium oxides ( $\text{Fe}_2\text{O}$  and  $\text{Al}_2\text{O}_3$ ) (Table 2). SEM-EDS analysis also  
285 indicated the dominance of Fe and Al (Figure S1 in the Supplementary Information).  
286 Titanium, Si, Ca and Na were also detected in the main composition. Prior to use in the  
287 column, there was a mineralogical dominance of the iron oxide hematite (as represented by H  
288 in Figure 1), detected at positions  $33.153$  and  $35.612^\circ 2\Theta$ , respectively (Figure 1). Rutile  
289 ( $\text{TiO}_2$ ) was also detected at position  $27.459^\circ 2\Theta$ . Following the column trials, XRD analysis  
290 was carried out on the spent media from both the DSW and forest run-off columns. New  
291 peaks were identified in the XRD patterns, as seen in Figure 1, which show the presence of P-  
292 based minerals, which were not present in the raw media. The new peaks detected in both the  
293 spent media following treatment of the DSW and forest run-off was calcium  
294 hydrogenphosphate (III) hydrate ( $\text{CaHPO}_4 \cdot 3\text{H}_2\text{O}$ ) at positions  $19.120$  and  $30.001^\circ 2\Theta$ . The  
295 presence of this mineral in the spent media indicates P retention within the bauxite residue  
296 after treatment. The particle size analysis (PSA) of the bauxite residue used in this study is  
297 shown in Table 3.

298

### 299 3.2 Influent and effluent water characterisation and rapid small-scale column study

300 The forest run-off had a pH of 7.57 and a DRP concentration of  $1.10 \text{ mg P L}^{-1}$ . The total  
301 phosphorus (TP) concentration of forest run-off is usually around  $1 \text{ mg L}^{-1}$  (Finnegan *et al.*,  
302 2012), whereas DSW has a TP concentration of 20 to  $100 \text{ mg L}^{-1}$  and a total nitrogen (TN)

303 concentration of 70 to 500 mg L<sup>-1</sup> (Minogue *et al.*, 2015). The DSW used in this study had a  
304 pH of 7.79 and a DRP concentration of 10.64 mg P L<sup>-1</sup>.

305

306 The BTC approached saturation much quicker for the DSW than for the forest run-off water  
307 (Figure 2). Similar to the findings of Vuković *et al.* (2011), the breakthrough time and  
308 exhaustion time increased with bed depth. As a result of its composition, there are other  
309 anions such as nitrates (NO<sub>3</sub><sup>-</sup>) and nitrites (NO<sub>2</sub><sup>-</sup>) present in the DSW (Ruane *et al.*, 2011),  
310 and therefore there is greater competitiveness for available adsorption sites and interferences  
311 between the adsorbent surface and the ions present in the aqueous solution. This may explain  
312 why the DSW-treating columns generated a BTC approaching saturation much faster than the  
313 bauxite residue columns treating forest run-off. When treating the forest run-off, the bauxite  
314 residue had a service time of approximately 22.80 min, based on the largest column before  
315 the initial breakthrough time of the bauxite residue occurred. However, when treating the  
316 DSW, it had a shorter service time of 5.80 min, as noted for the largest column before the  
317 initial breakthrough occurred. Taking into account the amount of bauxite residue used in the  
318 largest columns (21.16 and 20.78 g), this gives an estimated service time of 1.08 min g<sup>-1</sup>  
319 bauxite residue and 0.28 min g<sup>-1</sup> bauxite residue when treating forest run-off and DSW,  
320 respectively, before initial breakthrough (5%) would occur.

321

322 The modelled q<sub>t</sub> values were 0.27 mg P g<sup>-1</sup> media and 0.045 mg P g<sup>-1</sup> media when treating the  
323 DSW and forest run-off, respectively. These were lower than q<sub>t</sub> values of between 2.85 and  
324 8.74 mg P g<sup>-1</sup> for neutralised bauxite residue (Bauxol) used to treat secondary-treated  
325 wastewater (Despland *et al.*, 2011) and 25 mg P g<sup>-1</sup> for untreated bauxite residue used to treat  
326 synthetic water (Herron *et al.*, 2016) (Table 1). Compared to other studies that have used low-  
327 cost adsorbents such as zeolite (0.01 mg P g<sup>-1</sup> - Grace *et al.*, 2015) and granular ceramics (0.9

328 mg g<sup>-1</sup> - Chen *et al.*, 2012), the bauxite residue in the current study had a higher P  
329 adsorbency, but it was lower than crushed concrete (19.6 mg P g<sup>-1</sup> - Egemose *et al.*, 2012)  
330 and untreated biochar (32 mg P g<sup>-1</sup> - Wang *et al.*, 2015). It is important to note that full  
331 saturation of the bauxite residue was not reached in the current study and the wastewaters  
332 treated may have had an impact on the P adsorption capacity, as there may have been  
333 interferences and competition for adsorption sites due to the presence of other ions and  
334 contaminants in addition to the phosphate ions.

335

### 336 3.3 Speciation of P adsorbed

337 The adsorption of phosphate ions onto an adsorbent is measured by the decrease for  
338 phosphate in the influent after a certain amount of time (Loganathan *et al.*, 2014). Typically,  
339 the main mechanism of phosphate adsorption (and other anions and cations) onto the surface  
340 of iron and aluminium oxides may be separated into two processes: specific and non-specific  
341 adsorption (Stumm, 1992; Cornell and Schwertmann, 2003). Specific adsorption takes place  
342 through the process of ligand exchange (Jacukowicz-Sobala *et al.*, 2015). A phosphate ion  
343 exchanges with one or more hydroxyl groups, with the release of OH<sub>2</sub> and/or OH<sup>-</sup> back into  
344 the surrounding solution, contributing to the alkalisation of the surrounding environment  
345 (Cornell and Schwertmann, 2003), as shown in the following equations:

346



349

350 Non-specific adsorption, which was the main mechanism evident in this study, is inclusive of  
351 electrostatic interactions and surface precipitation (Loganathan *et al.*, 2014) between the  
352 surface of the sorbent and the phosphate ion (Jacukowicz-Sobala *et al.*, 2015). The

353 electrostatic interactions occur between the electric charge carried on the surface of the  
354 sorbent and type of ion present in the surrounding solution. Phosphate ions, which are of  
355 anionic nature, carry a negative charge, which interacts with the positive charge as carried by  
356 Ca, a cation (Loganathan *et al.*, 2014). Surface precipitation involves the formation of  
357 complexes/precipitates on the surface of the sorbent such as  $\text{CaHPO}_4^{3-}$  as a result of these ion  
358 interactions (Loganathan *et al.*, 2014). The adsorption of the phosphate ions is greatest in a  
359 low pH environment due to the abundance of positively charged sites (Jacukowicz-Sobala *et*  
360 *al.*, 2015).

361

362 X-ray diffraction and SEM analysis have been used in previous studies to show evidence of  
363 the presence of newly formed surface precipitates following the P adsorption process  
364 (Bowden *et al.*, 2009). The XRD data obtained in this study (Figure 1) show that the main  
365 interactions and complexes formed by the phosphate ions present in the wastewater (negative  
366 charge) were with Ca (positive charge) present in the bauxite residue, as evidenced by the  
367 presence of new peaks of  $\text{CaHPO}_4^{3-}$  in the XRD patterns following the treatment of both the  
368 DSW and forest run-off.. Depending on the pH of the solution, the species of P found in  
369 aqueous solution are  $\text{H}_3\text{PO}_4$  (pH < 4),  $\text{H}_2\text{PO}_4^-$  (pH ~ 0-9),  $\text{HPO}_4^{2-}$  (pH ~ 5-11) and  $\text{PO}_4^{3-}$  (pH  
370 >10) (Karageorgiou *et al.*, 2007; Despland *et al.*, 2011).

371

372 The FT-IR analysis of the bauxite residue media before and after treatment of both the DSW  
373 and forest run-off (Figures 3 and 4) indicated that similar changes occurred in the media  
374 following treatment of both wastewaters. Two distinct broad bands were detected between  
375 wavelength 600 to 900  $\text{cm}^{-1}$  and again at 1000 to 1400  $\text{cm}^{-1}$ . This was evident for both the  
376 DSW and forest run-off spent media. Intensive IR absorption bands are typically in the range  
377 of 560 to 600  $\text{cm}^{-1}$  and 1000 to 1100  $\text{cm}^{-1}$  for P species (Tejedor-Tejedor and Anderson, 1990;

378 Berzina-Cimdina and Borodajenko, 2012). However, it was not possible to identify specific  
379 P species due to some interferences, which are most likely due to the presence of many other  
380 ions present in each of the wastewater sources used.

381

382 There was an increase in the pH in the effluent for both the DSW and forest run-off treated  
383 wastewater (Figure 5). The influent pH of the DSW was 7.79, which increased to 8.94 in the  
384 40 cm column at  $t = 2$  hr. The influent pH of the forest run-off was 7.57 and increased to 8.81  
385 at  $t = 12$  hr in the 40 cm column. According to the Drinking Water Directive (98/83/EC), the  
386 pH value should be in the range of  $\geq 6.5$  and  $\leq 9.5$ . The values recorded in this study show  
387 that the pH values in the effluent are within this range, highlighting no potential risk to the  
388 surrounding environment.

389

#### 390 3.4 Trace metal and elemental analysis

391 Due to the complex nature of bauxite residue and its composition, there is potential for trace  
392 metal leaching to the surrounding environment (Despland *et al.*, 2011; Evans, 2016).

393 Pollution from metals can have an adverse and detrimental effect on the surrounding  
394 environment, affecting plant and animal life (Gomes *et al.*, 2016a; Olszewska *et al.*, 2017). In  
395 addition, the majority of metals that are in a soil environment are non-degradable (Guo *et al.*,  
396 2006).

397

398 The influent and effluent metal concentrations from the columns treating DSW and forest  
399 run-off, along with the parametric values, as mandated by the Irish EPA (2014), are displayed  
400 in Figures 6 and 7. In this study, the dominant species present in both effluents were Al and  
401 Fe, which were above the parametric values ( $0.2 \text{ mg L}^{-1}$  for both Al and Fe). Copper was  
402 released in both effluents, but did decrease with loading time when treating the DSW and the

403 level of Cu reduced to below the parametric value of 2 mg L<sup>-1</sup>. The level of Mn was lower in  
404 the effluent compared to the influent for all columns, showing a retention capacity within the  
405 column media, but it was higher than the parametric value of 0.05 mg L<sup>-1</sup>. Magnesium, Ga,  
406 V and Zn were also present in increased amounts in the effluent, due to leaching from the  
407 bauxite residue. However, the Mg and Zn did decrease with increasing loading time. There  
408 are currently no parametric values or EPA guideline values for drinking water parameters for  
409 Mg, Ga, V and Zn, although previous studies have highlighted that bauxite residue is  
410 inclusive of oxyanionic-forming elements, which are soluble at high pH range; these include  
411 Al, As, Cr, Mo and V (Mayes *et al.*, 2016). The main species of V present in bauxite residue  
412 was in the pentavalent form (Burke *et al.*, 2012, 2013), which may be problematic due to its  
413 toxicity (Burke *et al.*, 2012). Whilst V may be a potential issue (depending on the source of  
414 bauxite ore), it is also the focus of critical raw material (CRM) recovery studies (Gomes *et*  
415 *al.*, 2016b; Zhu *et al.*, 2018), which suggests the potential and need for further studies  
416 investigating the adsorbent potential of bauxite residue following the removal and recovery of  
417 CRMs such as V.

418

419 Previous work by Lopez *et al.* (1998) highlighted the ability of bauxite residue to retain Ni,  
420 Cu and Zn. Despland *et al.* (2014) showed that Bauxsol™ (neutralised bauxite residue  
421 produced using the Basecon™ procedure) had the ability to remove trace amounts of As, lead  
422 (Pb), Cd, Cr, Cu, Ni, Se, Zn, Mn and Al. This highlights the potential of bauxite residue in  
423 the removal of both cations and anions from aqueous solution. However, the composition and  
424 concentration of elements in bauxite will vary depending on the type of ore (Mayes *et al.*,  
425 2011).

426

427 Although there was overall evidence of mobilisation of some trace elements while treating  
428 the wastewater, one suggestion would be to include a rinse/wash period prior to packing the  
429 columns. This would reduce and/or eliminate the potential leaching of metals at the initial  
430 loading period and avoid further release as the loading period increases. Another option  
431 would be to apply a seawater treatment to the bauxite residue, which has been proven to  
432 lower the pH and therefore reduce the leaching of metal(loid) species (Cusack *et al.*, 2018;  
433 Johnston *et al.*, 2010).

434

#### 435 **4. Conclusions**

436

437 Several studies have focussed on the use of low-cost adsorbents in the removal of  
438 contaminants such as P from contaminated waters due to possible cost savings and to reutilise  
439 by-products from various sectors. This study demonstrated that bauxite residue has P  
440 (particularly dissolved reactive phosphorus) removal capabilities in both low (forest run-off)  
441 and high (dairy soiled water) range P-concentrated waters. The estimated service time of the  
442 column media before initial breakthrough, based on the performance of the largest columns,  
443 was 1.08 min g<sup>-1</sup> media for the forest run-off and 0.28 min g<sup>-1</sup> media for the dairy soiled  
444 water. Due to the composition of the bauxite residue, potential for metal(loid) leaching is a  
445 concern. Aluminium and iron were the dominant metals released in the treated effluent, but  
446 this may be eliminated by a preventative step such as introducing a washing period or a  
447 seawater neutralisation step prior to packing the bauxite residue into the columns.

448

#### 449 **Acknowledgements**

450 The authors would like to acknowledge the financial support of the Environmental Protection  
451 Agency (EPA) (2014-RE-MS-1).

452

453 **References**

454

455 Acelas, N.Y., Martin, B.D., López, D. and Jefferson, B., 2015. Selective removal of  
456 phosphate from wastewater using hydrated metal oxides dispersed within anionic exchange  
457 media. *Chemosphere 119*, 1353-1360. DOI Link:

458 <https://doi.org/10.1016/j.chemosphere.2014.02.024>

459

460 ÁdÁm, K., Sovik, A.K., Krogstad, T. and Heistad, A., 2007. Phosphorous removal by the  
461 filter materials light-weight aggregates and shellsand-a review of processes and experimental  
462 set-ups for improved design of filter systems for wastewater treatment. *Vatten 63*(3), 245.

463

464 Akhurst, D.J., Jones, G.B., Clark, M. and McConchie, D., 2006. Phosphate removal from  
465 aqueous solutions using neutralised bauxite refinery residues (Bauxsol™). *Environ. Chem.*  
466 *3*(1), 65-74. DOI Link: <https://doi.org/10.1071/EN05038>

467

468 Berzina-Cimdina, L. and Borodajenko, N., 2012. Research of calcium phosphates using  
469 Fourier transform infrared spectroscopy. In *Infrared Spectroscopy-Materials Science,*  
470 *Engineering and Technology*. InTech. Available:

471 [http://scholar.google.com/scholar\\_url?url=https%3A%2F%2Fwww.intechopen.com%2Fdownload%2Fpdf%2F36171&hl=en&sa=T&oi=ggp&ct=res&cd=0&d=1876013532413993455&ei=JQ5fW6ODB4SQmwHoq7O4BA&scisig=AAGBfm0zcrG1iAsbV5Fv1kKQs9aPk9QMN](http://scholar.google.com/scholar_url?url=https%3A%2F%2Fwww.intechopen.com%2Fdownload%2Fpdf%2F36171&hl=en&sa=T&oi=ggp&ct=res&cd=0&d=1876013532413993455&ei=JQ5fW6ODB4SQmwHoq7O4BA&scisig=AAGBfm0zcrG1iAsbV5Fv1kKQs9aPk9QMN)  
472 [A&nossl=1&ws=1440x845](http://scholar.google.com/scholar_url?url=https%3A%2F%2Fwww.intechopen.com%2Fdownload%2Fpdf%2F36171&hl=en&sa=T&oi=ggp&ct=res&cd=0&d=1876013532413993455&ei=JQ5fW6ODB4SQmwHoq7O4BA&scisig=AAGBfm0zcrG1iAsbV5Fv1kKQs9aPk9QMN) [accessed 30.07.2018].

475

476 Bhatnagar, A., Vilar, V.J., Botelho, C.M. and Boaventura, R.A., 2011. A review of the use of  
477 red mud as adsorbent for the removal of toxic pollutants from water and wastewater. *Environ.*  
478 *Technol.* 32(3), 231-249. DOI Link: <https://doi.org/10.1080/09593330.2011.560615>  
479

480 Bowden, L.I., Jarvis, A.P., Younger, P.L. and Johnson, K.L., 2009. Phosphorus removal from  
481 waste waters using basic oxygen steel slag. *Environmental science & technology*, 43(7),  
482 pp.2476-2481.  
483

484 Brennan, R.B., Wall, D., Fenton, O., Grant, J., Sharpley, A.N. and Healy, M.G., 2014. The  
485 impact of chemical amendment of dairy cattle slurry before land application on soil  
486 phosphorus dynamics. *Commun. Soil Sci. Plant Anal.* 45(16), 2215 – 2233. DOI Link:  
487 <http://dx.doi.org/10.1080/00103624.2014.912293>  
488

489 Bridger, S. and Knowles, M., 2000. A complete method for environmental samples by  
490 simultaneous axially viewed ICP-AES following USEPA guidelines. Varian ICP-OES At  
491 Work (29) Available: <https://www.agilent.com/cs/library/applications/ICPES-29.pdf>  
492 [24.05.2018].  
493

494 Burke, I.T., Mayes, W.M., Peacock, C.L., Brown, A.P., Jarvis, A.P. and Gruiz, K., 2012.  
495 Speciation of arsenic, chromium, and vanadium in red mud samples from the Ajka spill site,  
496 Hungary. *Environ. Sci. Technol.* 46(6), 3085-3092. DOI Link: 10.1021/es3003475  
497

498 Burke, I.T., Peacock, C.L., Lockwood, C.L., Stewart, D.I., Mortimer, R.J., Ward, M.B.,  
499 Renforth, P., Gruiz, K. and Mayes, W.M., 2013. Behavior of aluminum, arsenic, and

500 vanadium during the neutralization of red mud leachate by HCl, gypsum, or seawater.  
501 *Environ. Sci. Technol.* 47(12), 6527-6535. DOI Link: 10.1021/es4010834  
502  
503 Callery, O., Brennan, R.B. and Healy, M.G., 2015. Use of amendments in a peat soil to  
504 reduce phosphorus losses from forestry operations. *Ecol. Eng.* 85, 193 – 200. DOI Link:  
505 <https://doi.org/10.1016/j.ecoleng.2015.10.016>  
506  
507 Callery, O., Healy, M.G., Rognard, F., Barthelemy, L. and Brennan, R.B., 2016. Evaluating  
508 the long-term performance of low-cost adsorbents using small-scale adsorption column  
509 experiments. *Water Res.* 101, 429-440. DOI Link:  
510 <https://doi.org/10.1016/j.watres.2016.05.093>  
511  
512 Callery, O. and Healy, M.G., 2017. Predicting the propagation of concentration and  
513 saturation fronts in fixed-bed filters. *Water Res.* 123, 556-568. DOI Link:  
514 <https://doi.org/10.1016/j.watres.2017.07.010>  
515  
516 Castaldi, P., Silveti, M., Enzo, S. and Melis, P., 2010. Study of sorption processes and FT-IR  
517 analysis of arsenate sorbed onto red muds (a bauxite ore processing waste). *J. Hazard. Mater.*  
518 175(1-3), 172-178. DOI Link: <https://doi.org/10.1016/j.jhazmat.2009.09.145>  
519  
520 Castaldi, P., Silveti, M., Enzo, S. and Deiana, S., 2011. X-ray diffraction and thermal  
521 analysis of bauxite ore-processing waste (red mud) exchanged with arsenate and phosphate.  
522 *Clays Clay Miner.* 59(2), 189-199. DOI Link: <https://doi.org/10.1346/CCMN.2011.0590207>  
523

524 Chen, J.P., Yoon, J.T. and Yiacoumi, S., 2003. Effects of chemical and physical properties of  
525 influent on copper sorption onto activated carbon fixed-bed columns. *Carbon* 41(8), 1635-  
526 1644. DOI Link: [https://doi.org/10.1016/S0008-6223\(03\)00117-9](https://doi.org/10.1016/S0008-6223(03)00117-9)  
527

528 Chen, N., Feng, C., Zhang, Z., Liu, R., Gao, Y., Li, M., Sugiura, N., 2012. Preparation and  
529 characterization of lanthanum (III) loaded granular ceramic for phosphorus adsorption from  
530 aqueous solution. *J. Taiwan Instit. Chem. Eng.* 43, 783-789. DOI Link:  
531 <https://doi.org/10.1016/j.jtice.2012.04.003>  
532

533 Claveau-Mallet, D., Wallace, S. and Comeau, Y., 2013. Removal of phosphorus, fluoride and  
534 metals from a gypsum mining leachate using steel slag filters. *Water Res.* 47(4), 1512-1520.  
535 DOI Link: <https://doi.org/10.1016/j.watres.2012.11.048>  
536

537 Cordell, D. and White, S., 2011. Peak phosphorus: clarifying the key issues of a vigorous  
538 debate about long-term phosphorus security. *Sustainability* 3(10), 2027-2049. DOI Link:  
539 <https://doi.org/10.3390/su3102027>  
540

541 Cornell, R.M. and Schwertmann, U., 2003. *The iron oxides: structure, properties, reactions,*  
542 *occurrences and uses.* John Wiley & Sons. Available:  
543 [https://books.google.ie/books?hl=en&lr=&id=dIMuE3\\_klW4C&oi=fnd&pg=PA1&dq=Cornell,+R.M.+and+Schwertmann,+U.,+2003.+The+iron+oxides:+structure,+properties,+reactions,+occurrences+and+uses.+John+Wiley+%26+Sons.&ots=l0jQWg\\_4gN&sig=kNxJyUHBF3-UemiW-s\\_EvlaeCs&redir\\_esc=y#v=onepage&q=Cornell%2C%20R.M.%20and%20Schwertmann%2C%20U.%2C%202003.%20The%20iron%20oxides%3A%20structure%2C%20properties%2](https://books.google.ie/books?hl=en&lr=&id=dIMuE3_klW4C&oi=fnd&pg=PA1&dq=Cornell,+R.M.+and+Schwertmann,+U.,+2003.+The+iron+oxides:+structure,+properties,+reactions,+occurrences+and+uses.+John+Wiley+%26+Sons.&ots=l0jQWg_4gN&sig=kNxJyUHBF3-UemiW-s_EvlaeCs&redir_esc=y#v=onepage&q=Cornell%2C%20R.M.%20and%20Schwertmann%2C%20U.%2C%202003.%20The%20iron%20oxides%3A%20structure%2C%20properties%2)  
544 [s,+occurrences+and+uses.+John+Wiley+%26+Sons.&ots=l0jQWg\\_4gN&sig=kNxJyUHBF3-UemiW-](https://books.google.ie/books?hl=en&lr=&id=dIMuE3_klW4C&oi=fnd&pg=PA1&dq=Cornell,+R.M.+and+Schwertmann,+U.,+2003.+The+iron+oxides:+structure,+properties,+reactions,+occurrences+and+uses.+John+Wiley+%26+Sons.&ots=l0jQWg_4gN&sig=kNxJyUHBF3-UemiW-s_EvlaeCs&redir_esc=y#v=onepage&q=Cornell%2C%20R.M.%20and%20Schwertmann%2C%20U.%2C%202003.%20The%20iron%20oxides%3A%20structure%2C%20properties%2)  
545 [s\\_EvlaeCs&redir\\_esc=y#v=onepage&q=Cornell%2C%20R.M.%20and%20Schwertmann%2C%20U.%2C%202003.%20The%20iron%20oxides%3A%20structure%2C%20properties%2](https://books.google.ie/books?hl=en&lr=&id=dIMuE3_klW4C&oi=fnd&pg=PA1&dq=Cornell,+R.M.+and+Schwertmann,+U.,+2003.+The+iron+oxides:+structure,+properties,+reactions,+occurrences+and+uses.+John+Wiley+%26+Sons.&ots=l0jQWg_4gN&sig=kNxJyUHBF3-UemiW-s_EvlaeCs&redir_esc=y#v=onepage&q=Cornell%2C%20R.M.%20and%20Schwertmann%2C%20U.%2C%202003.%20The%20iron%20oxides%3A%20structure%2C%20properties%2)  
546 [-UemiW-](https://books.google.ie/books?hl=en&lr=&id=dIMuE3_klW4C&oi=fnd&pg=PA1&dq=Cornell,+R.M.+and+Schwertmann,+U.,+2003.+The+iron+oxides:+structure,+properties,+reactions,+occurrences+and+uses.+John+Wiley+%26+Sons.&ots=l0jQWg_4gN&sig=kNxJyUHBF3-UemiW-s_EvlaeCs&redir_esc=y#v=onepage&q=Cornell%2C%20R.M.%20and%20Schwertmann%2C%20U.%2C%202003.%20The%20iron%20oxides%3A%20structure%2C%20properties%2)  
547 [s\\_EvlaeCs&redir\\_esc=y#v=onepage&q=Cornell%2C%20R.M.%20and%20Schwertmann%2C%20U.%2C%202003.%20The%20iron%20oxides%3A%20structure%2C%20properties%2](https://books.google.ie/books?hl=en&lr=&id=dIMuE3_klW4C&oi=fnd&pg=PA1&dq=Cornell,+R.M.+and+Schwertmann,+U.,+2003.+The+iron+oxides:+structure,+properties,+reactions,+occurrences+and+uses.+John+Wiley+%26+Sons.&ots=l0jQWg_4gN&sig=kNxJyUHBF3-UemiW-s_EvlaeCs&redir_esc=y#v=onepage&q=Cornell%2C%20R.M.%20and%20Schwertmann%2C%20U.%2C%202003.%20The%20iron%20oxides%3A%20structure%2C%20properties%2)  
548 [C%20U.%2C%202003.%20The%20iron%20oxides%3A%20structure%2C%20properties%2](https://books.google.ie/books?hl=en&lr=&id=dIMuE3_klW4C&oi=fnd&pg=PA1&dq=Cornell,+R.M.+and+Schwertmann,+U.,+2003.+The+iron+oxides:+structure,+properties,+reactions,+occurrences+and+uses.+John+Wiley+%26+Sons.&ots=l0jQWg_4gN&sig=kNxJyUHBF3-UemiW-s_EvlaeCs&redir_esc=y#v=onepage&q=Cornell%2C%20R.M.%20and%20Schwertmann%2C%20U.%2C%202003.%20The%20iron%20oxides%3A%20structure%2C%20properties%2)

549 [C%20reactions%2C%20occurrences%20and%20uses.%20John%20Wiley%20%26%20Sons.](#)  
550 [&f=false](#) [accessed 11.09.2018].  
551  
552 Courtney, R. and Harrington, T., 2010. Assessment of plant-available phosphorus in a fine  
553 textured sodic substrate. *Ecol. Eng.* 36(4), 542-547. DOI Link:  
554 <https://doi.org/10.1016/j.ecoleng.2009.12.001>  
555  
556 Cusack, P.B., Healy, M.G., Ryan, P.C., Burke, I.T., O'Donoghue, L.M., Ujaczki, É. and  
557 Courtney, R., 2018. Enhancement of bauxite residue as a low-cost adsorbent for phosphorus  
558 in aqueous solution, using seawater and gypsum treatments. *J. Clean Prod.* 179, 217-224.  
559 DOI Link: <https://doi.org/10.1016/j.jclepro.2018.01.092>  
560  
561 De Gisi, S., Lofrano, G., Grassi, M. and Notarnicola, M., 2016. Characteristics and  
562 adsorption capacities of low-cost sorbents for wastewater treatment: a review. *Sustainable*  
563 *Mater. Technol.* 9, 10-40. DOI Link: <https://doi.org/10.1016/j.susmat.2016.06.002>  
564  
565 Despland, L.M., Clark, M.W., Vancov, T., Erler, D. and Aragno, M., 2011. Nutrient and  
566 trace-metal removal by Bauxsol pellets in wastewater treatment. *Environ. Sci. Technol.*  
567 45(13), 5746-5753. DOI Link: <https://doi.org/10.1021/es200934y>  
568  
569 Despland, L.M., Clark, M.W., Vancov, T. and Aragno, M., 2014. Nutrient removal and  
570 microbial communities' development in a young unplanted constructed wetland using  
571 Bauxsol™ pellets to treat wastewater. *Sci. Total Environ.* 484, 167-175. DOI Link:  
572 <https://doi.org/10.1016/j.scitotenv.2014.03.030>  
573

574 Egemose, S., Sønderup, M.J., Beinthin, M.V., Reitzel, K., Hoffmann, C.C., Flindt, M.R.,  
575 2012. Crushed concrete as a phosphate binding material: a potential new management tool. *J.*  
576 *Environ. Qual.* 41, 647-653. DOI Link: <https://doi.org/10.2134/jeq2011.0134>.

577

578 EPA, 2014. Drinking Water Parameters Microbiological, Chemical and Indicator Parameters  
579 in the 2014 Drinking Water Regulations. Available:  
580 [www.epa.ie/pubs/advice/drinkingwater/2015\\_04\\_21\\_ParametersStandaloneDoc.pdf](http://www.epa.ie/pubs/advice/drinkingwater/2015_04_21_ParametersStandaloneDoc.pdf)  
581 [accessed 29.05.2018].

582

583 European Drinking Water Directive (Council Directive 98/83/EC of 3 November 1998 on the  
584 quality of water intended for human consumption) (1998). Available: [https://eur-](https://eur-lex.europa.eu/legal-content/EN/TXT/PDF/?uri=CELEX:31998L0083&from=EN)  
585 [lex.europa.eu/legal-content/EN/TXT/PDF/?uri=CELEX:31998L0083&from=EN](https://eur-lex.europa.eu/legal-content/EN/TXT/PDF/?uri=CELEX:31998L0083&from=EN) [accessed  
586 20.07.2018].

587

588 Evans, K., 2016. The history, challenges, and new developments in the management and use  
589 of bauxite residue. *J. Sustainable Metallurgy* 2(4), 316-331. DOI Link:  
590 <https://doi.org/10.1007/s40831-016-0060-x>

591

592 Fenton, O., Healy, M.G., Rodgers, M. 2009. Use of ochre from an abandoned metal mine in  
593 the south east of Ireland for phosphorus sequestration from dairy dirty water. *J. Environ.*  
594 *Qual.* 38, 1120 – 1125. DOI Link: <https://doi.org/10.2134/jeq2008.0227>

595

596 Finnegan, J., Regan, J.T., De Eyto, E., Ryder, E., Tiernan, D. and Healy, M.G., 2012.  
597 Nutrient dynamics in a peatland forest riparian buffer zone and implications for the

598 establishment of planted saplings. *Ecol. Eng.* 47, 155-164. DOI Link:  
599 <https://doi.org/10.1016/j.ecoleng.2012.06.023>  
600  
601 García-Mateos, F.J., Ruiz-Rosas, R., Marqués, M.D., Cotoruelo, L.M., Rodríguez-Mirasol, J.  
602 and Cordero, T., 2015. Removal of paracetamol on biomass-derived activated carbon:  
603 modeling the fixed bed breakthrough curves using batch adsorption experiments. *Chem. Eng.*  
604 *J.* 279, 18-30. DOI Link: <https://doi.org/10.1016/j.cej.2015.04.144>  
605  
606 Ge, H., Batstone, D.J. and Keller, J., 2015. Biological phosphorus removal from abattoir  
607 wastewater at very short sludge ages mediated by novel PAO clade Comamonadaceae. *Water*  
608 *Res.* 69, 173-182. DOI Link: <https://doi.org/10.1016/j.watres.2014.11.026>  
609  
610 Gomes, H.I., Mayes, W.M., Rogerson, M., Stewart, D.I. and Burke, I.T., 2016. Alkaline  
611 residues and the environment: a review of impacts, management practices and opportunities.  
612 *J. Clean Prod.* 112, 3571-3582. DOI Link: <https://doi.org/10.1016/j.jclepro.2015.09.111>  
613  
614 Gomes, H.I., Jones, A., Rogerson, M., Burke, I.T. and Mayes, W.M., 2016. Vanadium  
615 removal and recovery from bauxite residue leachates by ion exchange. *Environ. Sci. Poll.*  
616 *Res.* 23(22), 23034-23042. DOI Link: <https://doi.org/10.1007/s11356-016-7514-3>  
617  
618 Grace, M.A., Healy, M.G. and Clifford, E., 2015. Use of industrial by-products and natural  
619 media to adsorb nutrients, metals and organic carbon from drinking water. *Sci. Total Environ.*  
620 518, 491-497. DOI Link: <https://doi.org/10.1016/j.scitotenv.2015.02.075>  
621

622 Grace, M.A., Clifford, E. and Healy, M.G., 2016. The potential for the use of waste products  
623 from a variety of sectors in water treatment processes. *J. Clean Prod.* 137, 788-802. DOI  
624 Link: <https://doi.org/10.1016/j.jclepro.2016.07.113>  
625

626 Gräfe, M., Power, G. and Klauber, C., 2011. Bauxite residue issues: III. Alkalinity and  
627 associated chemistry. *Hydrometallurgy*, 108(1-2), 60-79. DOI Link:  
628 <https://doi.org/10.1016/j.hydromet.2011.02.004>  
629

630 Guo, G., Zhou, Q. and Ma, L.Q., 2006. Availability and assessment of fixing additives for the  
631 in situ remediation of heavy metal contaminated soils: a review. *Environ. Monit. Assess.*  
632 116(1-3), 513-528. DOI Link: <https://doi.org/10.1007/s10661-006-7668-4>  
633

634 Hauduc, H., Takács, I., Smith, S., Szabo, A., Murthy, S., Daigger, G.T. and Spérandio, M.,  
635 2015. A dynamic physicochemical model for chemical phosphorus removal. *Water Res.* 73,  
636 157-170. DOI Link: <https://doi.org/10.1016/j.watres.2014.12.053>  
637

638 Herron, S.L., Sharpley, A.N., Brye, K.R. and Miller, D.M., 2016. Optimizing hydraulic and  
639 chemical properties of iron and aluminum byproducts for use in on-farm containment  
640 structures for phosphorus removal. *J. Environ. Protection* 7(12), 1835. DOI Link:  
641 <https://doi.org/10.4236/jep.2016.712146>  
642

643 Huang, W., Wang, S., Zhu, Z., Li, L., Yao, X., Rudolph, V. and Haghseresht, F., 2008.  
644 Phosphate removal from wastewater using red mud. *J. Hazard. Mater.* 158(1), 35-42. DOI  
645 Link: <https://doi.org/10.1016/j.jhazmat.2008.01.061>  
646

647 Jacukowicz-Sobala, I., Ociński, D. and Kociołek-Balawejder, E., 2015. Iron and aluminium  
648 oxides containing industrial wastes as adsorbents of heavy metals: application possibilities  
649 and limitations. *Waste Manage. Res.* 33(7), 612-629. DOI Link:  
650 <https://doi.org/10.1177/0734242X15584841>  
651

652 Johnston, M., Clark, M.W., McMahon, P. and Ward, N., 2010. Alkalinity conversion of  
653 bauxite refinery residues by neutralization. *J. Hazard. Mater.* 182(1-3), 710-715. DOI Link:  
654 <https://doi.org/10.1016/j.jhazmat.2010.06.091>  
655

656 Karageorgiou, K., Paschalis, M. and Anastassakis, G.N., 2007. Removal of phosphate species  
657 from solution by adsorption onto calcite used as natural adsorbent. *J. Hazard. Mater.* 139(3),  
658 447-452. DOI Link: <https://doi.org/10.1016/j.jhazmat.2006.02.038>  
659

660 Kong, X., Li, M., Xue, S., Hartley, W., Chen, C., Wu, C., Li, X. and Li, Y., 2017. Acid  
661 transformation of bauxite residue: conversion of its alkaline characteristics. *J. Hazard. Mater.*  
662 324, 382-390. DOI Link: <https://doi.org/10.1016/j.jhazmat.2016.10.073>  
663

664 Lalley, J., Han, C., Mohan, G.R., Dionysiou, D.D., Speth, T.F., Garland, J. and Nadagouda,  
665 M.N., 2015. Phosphate removal using modified Bayoxide® E33 adsorption media. *Environ.*  
666 *Sci. Water Res. Technol.* 1(1), 96-107. DOI Link: <https://doi.org/10.1039/C4EW00020J>  
667

668 Liu, Y., Lin, C. and Wu, Y., 2007. Characterization of red mud derived from a combined  
669 Bayer Process and bauxite calcination method. *J. Hazard. Mater.* 146, 255-261. DOI Link:  
670 <https://doi.org/10.1016/j.jhazmat.2006.12.015>  
671

672 Loganathan, P., Vigneswaran, S., Kandasamy, J. and Bolan, N.S., 2014. Removal and  
673 recovery of phosphate from water using sorption. *Critical Reviews in Environmental Science*  
674 *and Technology*, 44(8), pp.847-907.

675

676 Lopez, E., Soto, B., Arias, M., Nunez, A., Rubinos, D. and Barral, M.T., 1998. Adsorbent  
677 properties of red mud and its use for wastewater treatment. *Water Res.* 32, 1314-1322. DOI

678 Link: [https://doi.org/10.1016/S0043-1354\(97\)00326-6](https://doi.org/10.1016/S0043-1354(97)00326-6)

679

680 Mayes, W.M., Jarvis, A.P., Burke, I.T., Walton, M., Feigl, V., Klebercz, O. and Gruiz, K.,  
681 2011. Dispersal and attenuation of trace contaminants downstream of the Ajka bauxite  
682 residue (red mud) depository failure, Hungary. *Environ. Sci. Technol.* 45(12), 5147-5155.

683 DOI Link: <https://doi.org/10.1021/es200850y>

684

685 Mayes, W.M., Burke, I.T., Gomes, H.I., Anton, Á.D., Molnár, M., Feigl, V. and Ujaczki, É.,  
686 2016. Advances in understanding environmental risks of red mud after the Ajka spill,  
687 Hungary. *J. Sustainable Metallurgy* 2(4), 332-343. DOI Link:

688 <https://doi.org/10.1007/s40831-016-0050-z>

689

690 McConchie, D., Clark, M., Davies-McConchie, F., 2001. Processes and Compositions for  
691 Water Treatment, Neauveau Technology Investments, Australian, p. 28.

692

693 Minogue, D., French, P., Bolger, T. and Murphy, P.N.C., 2015. Characterisation of dairy  
694 soiled water in a survey of 60 Irish dairy farms. *Irish J. Agricultural and Food Res.* 54(1), 1-

695 16. DOI Link: <https://doi.org/10.1515/ijaf-2015-0001>

696

697 Murnane, J.G., Brennan, R.B., Fenton, O. and Healy, M.G., 2016. Zeolite combined with  
698 alum and aluminium chloride mixed with agricultural slurries reduces carbon losses in runoff  
699 from grassed soil boxes. *J. Environ. Qual.* 44(5), 1674 – 1683. DOI Link:  
700 <https://doi.org/10.2134/jeq2016.05.0175>  
701  
702 Nowak, B., Aschenbrenner, P. and Winter, F., 2013. Heavy metal removal from sewage  
703 sludge ash waste fly ash—a comparison. *Fuel Process. Technol.* 105, 195-201. DOI Link:  
704 <https://doi.org/10.1016/j.fuproc.2011.06.027>  
705  
706 O’Flynn, C.J., Fenton, O., Wall, D., Brennan, R.B., McLaughlin, M.J. and Healy, M.G.,  
707 2018. Influence of soil phosphorus status, texture, pH and metal content on the efficacy of  
708 amendments to pig slurry in reducing phosphorus losses. *Soil Use and Management* 34(1), 1-  
709 8. DOI Link: <https://doi.org/10.1111/sum.12391>  
710  
711 Olszewska, J.P., Heal, K.V., Winfield, I.J., Eades, L.J. and Spears, B.M., 2017. Assessing the  
712 role of bed sediments in the persistence of red mud pollution in a shallow lake (Kinghorn  
713 Loch, UK). *Water Res.* 123, 569-577. DOI Link: <https://doi.org/10.1016/j.watres.2017.07.009>  
714  
715 Pan, G., Lyu, T. and Mortimer, R., 2018. Comment: closing phosphorus cycle from natural  
716 waters: re-capturing phosphorus through an integrated water-energy-food strategy. DOI  
717 Link: <https://doi.org/10.1016/j.jes.2018.02.018>.  
718  
719 Penn, C., McGrath, J., Bowen, J. and Wilson, S., 2014. Phosphorus removal structures: A  
720 management option for legacy phosphorus. *J. Soil Water Conserv.* 69(2), 51A-56A. DOI  
721 Link: <https://doi.org/10.2489/jswc.69.2.51A>

722

723 Pratt, C., Parsons, S.A., Soares, A. and Martin, B.D., 2012. Biologically and chemically  
724 mediated adsorption and precipitation of phosphorus from wastewater. *Curr. Opin.*  
725 *Biotechnol.* 23(6), 890-896. DOI Link: <https://doi.org/10.1016/j.copbio.2012.07.003>

726

727 Pretty, J. and Bharucha, Z.P., 2014. Sustainable intensification in agricultural systems.  
728 *Annals of Botany* 114(8), 1571-1596. DOI Link: <https://doi.org/10.1093/aob/mcu205>

729

730 Ruane, E.M., Murphy, P.N., Healy, M.G., French, P. and Rodgers, M., 2011. On-farm  
731 treatment of dairy soiled water using aerobic woodchip filters. *Water Res.* 45(20), 6668-6676.  
732 DOI Link: <https://doi.org/10.1016/j.watres.2011.09.055>

733

734 Sharpley, A., 2016. Managing agricultural phosphorus to minimize water quality impacts.  
735 *Scientia Agricola* 73(1), 1-8. DOI Link: <http://dx.doi.org/10.1590/0103-9016-2015-0107>

736

737 Søvik, A.K. and Kløve, B., 2005. Phosphorus retention processes in shell sand filter systems  
738 treating municipal wastewater. *Ecol. Eng.* 25(2), 168-182. DOI Link:

739 <https://doi.org/10.1016/j.ecoleng.2005.04.007>

740

741 Stumm, W., 1992. *Chemistry of the solid-water interface: processes at the mineral-water and*  
742 *particle-water interface in natural systems*. John Wiley & Son Inc..

743

744 Sukačová, K., Trtílek, M. and Rataj, T., 2015. Phosphorus removal using a microalgal  
745 biofilm in a new biofilm photobioreactor for tertiary wastewater treatment. *Water Res.* 71,

746 55-63. DOI Link: <https://doi.org/10.1016/j.watres.2014.12.049>

747

748 Tejedor-Tejedor, M.I. and Anderson, M.A., 1990. The protonation of phosphate on the  
749 surface of goethite as studied by CIR-FTIR and electrophoretic mobility. *Langmuir* 6(3), 602-  
750 611. DOI Link: [http://doi.org/0743-7463/90/2406-0602\\$02.50/0](http://doi.org/0743-7463/90/2406-0602$02.50/0)

751

752 Tresintsi, S., Simeonidis, K., Katsikini, M., Paloura, E.C., Bantsis, G. and Mitrakas, M.,  
753 2014. A novel approach for arsenic adsorbents regeneration using MgO. *J. Hazard. Mater.*  
754 265, 217-225. DOI Link: <https://doi.org/10.1016/j.jhazmat.2013.12.003>

755

756 Ujaczki, É., Feigl, V., Molnár, M., Cusack, P., Curtin, T., Courtney, R., O'Donoghue, L.,  
757 Davris, P., Hugi, C., Evangelou, M.W. and Balomenos, E., (2018). Re-using bauxite  
758 residues: benefits beyond (critical raw) material recovery. *Journal of Chemical Technology &*  
759 *Biotechnology* 93(9), 2498-510. DOI Link: <https://doi.org/10.1002/jctb.5687>

760

761 United Nations. 2015. Transforming our world: the 2030 agenda for sustainable development.

762 Available:

763 [http://www.un.org/en/development/desa/population/migration/generalassembly/docs/globalco](http://www.un.org/en/development/desa/population/migration/generalassembly/docs/globalcompact/A_RES_70_1_E.pdf)  
764 [mpact/A\\_RES\\_70\\_1\\_E.pdf](http://www.un.org/en/development/desa/population/migration/generalassembly/docs/globalcompact/A_RES_70_1_E.pdf) [accessed 18.07.2018].

765

766 Vuković, G.D., Marinković, A.D., Škapin, S.D., Ristić, M.Đ., Aleksić, R., Perić-Grujić, A.A.  
767 and Uskoković, P.S., 2011. Removal of lead from water by amino modified multi-walled  
768 carbon nanotubes. *Chem. Eng. J.* 173(3), 855-865. DOI Link:  
769 <https://doi.org/10.1016/j.cej.2011.08.036>

770

771 Wang, B., Lehmann, J., Hanley, K., Hestrin, R., Enders, A., 2015. Adsorption and desorption  
772 of ammonium by maple wood biochar as a function of oxidation and  
773 pH. *Chemosphere* 138,120-126. DOI Link:  
774 <https://doi.org/10.1016/j.chemosphere.2015.05.062>.

775

776 Wang, X.X., Wu, Y.H., Zhang, T.Y., Xu, X.Q., Dao, G.H. and Hu, H.Y., 2016. Simultaneous  
777 nitrogen, phosphorous, and hardness removal from reverse osmosis concentrate by  
778 microalgae cultivation. *Water Res.* 94, 215-224. DOI Link:  
779 <https://doi.org/10.1016/j.watres.2016.02.062>

780

781 Weissert, C. and Kehr, J., 2018. Macronutrient sensing and signaling in plants. In *Plant*  
782 *Macronutrient Use Efficiency* (45-64). DOI Link: [https://doi.org/10.1016/B978-0-12-](https://doi.org/10.1016/B978-0-12-811308-0.00003-X)  
783 [811308-0.00003-X](https://doi.org/10.1016/B978-0-12-811308-0.00003-X)

784

785 Wu, K., Chen, Y., Ouyang, Y., Lei, H. and Liu, T., 2018. Adsorptive removal of fluoride  
786 from water by granular zirconium–aluminum hybrid adsorbent: performance and  
787 mechanisms. *Environ. Sci. Pollution Res.* 25(16),15390-403. DOI Link:  
788 <https://doi.org/10.1007/s11356-018-1711-1>

789

790 Ye, J., Zhang, P., Hoffmann, E., Zeng, G., Tang, Y., Dresely, J., Liu, Y., 2014. Comparison  
791 of response surface methodology and artificial neural network in optimization and prediction  
792 of acid activation of Bauxsol for phosphorus adsorption. *Water, Air, Soil Pollut.* 225(12),  
793 2225. DOI Link: <https://doi.org/10.1007/s11270-014-2225-1>

794

795 Zhou, Z., Hu, D., Ren, W., Zhao, Y., Jiang, L.M. and Wang, L., 2015. Effect of humic  
796 substances on phosphorus removal by struvite precipitation. *Chemosphere* 141, 94-99. DOI  
797 Link: <https://doi.org/10.1016/j.chemosphere.2015.06.089>  
798

799 Zhou, B., Xu, Y., Vogt, R.D., Lu, X., Li, X., Deng, X., Yue, A. and Zhu, L., 2016. Effects of  
800 land use change on phosphorus levels in surface waters—a case study of a watershed strongly  
801 influenced by agriculture. *Water, Air, Soil Pollut.* 227(5), 160. DOI Link:  
802 <https://doi.org/10.1007/s11270-016-2855-6>  
803

804 Zhu, F., Li, Y., Xue, S., Hartley, W. and Wu, H., 2016. Effects of iron-aluminium oxides and  
805 organic carbon on aggregate stability of bauxite residues. *Environ. Sci. Pollution Res.* 23(9),  
806 9073-9081. DOI Link: <https://doi.org/10.1007/s11356-016-6172-9>  
807

808 Zhu, X., Li, W., Zhang, Q., Zhang, C. and Chen, L., 2018. Separation characteristics of  
809 vanadium from leach liquor of red mud by ion exchange with different resins.  
810 *Hydrometallurgy* 176, 42-48. DOI Link: <https://doi.org/10.1016/j.hydromet.2018.01.009>  
811  
812  
813  
814  
815  
816  
817  
818  
819

820  
821

**Table 1** Phosphorus (P) adsorption studies that have been carried out using bauxite residue, untreated and treated residues, and their recovery efficiencies (adapted from Cusack *et al.*, 2018).

	<b>P recovery technique</b>	<b>Factors investigated</b>	<b>Type of water</b>	<b>Initial P concentration of the water</b>	<b>P recovered</b>	<b>Reference</b>
<b>Untreated bauxite residue</b>	Batch adsorption experiment	Kinetics, pH and temperature	Synthetic water	5-100 mg P L <sup>-1</sup>	0.20 mg P g <sup>-1</sup>	Grace <i>et al.</i> , 2015
<b>Untreated bauxite residue</b>	Column study	Initial concentration, particle size	Synthetic water	60-1000 mg P L <sup>-1</sup>	25 mg P g <sup>-1*</sup>	Herron <i>et al.</i> , 2016
<b>Untreated bauxite residue</b>	Batch adsorption experiment	Initial concentration, pH, particle size	Synthetic water	10-150 mg P L <sup>-1</sup>	0.345-1 mg P g <sup>-1</sup>	Cusack <i>et al.</i> , 2018
<b>Gypsum Treated</b>	Batch adsorption experiment	Contact time	Synthetic water	20-400 mg P L <sup>-1</sup>	7.03 mg P g <sup>-1</sup>	Lopez <i>et al.</i> , 1998
<b>Gypsum Treated</b>	Batch adsorption experiment	Initial concentration, pH, particle size	Synthetic water	10-150 mg P L <sup>-1</sup>	1.39-2.73 mg P g <sup>-1</sup>	Cusack <i>et al.</i> , 2018
<b>Seawater Treated</b>	Batch adsorption experiment	Initial concentration, pH, particle size	Synthetic water	10-150 mg P L <sup>-1</sup>	0.48-1.92 mg P g <sup>-1</sup>	Cusack <i>et al.</i> , 2018
<b>Brine treated bauxite residue (Bauxsol™**)</b>	Batch adsorption experiment	pH, ionic strength, time	Synthetic water	0.5-2 mg P L <sup>-1</sup>	6.5-14.9 mg P g <sup>-1</sup>	Akhurst <i>et al.</i> , 2006
<b>Brine treated bauxite residue (Bauxsol™**)</b>	Column study	Kinetics, particle size	Secondary treated effluent	3-9.2 mg P L <sup>-1</sup>	2.85-8.74 mg P g <sup>-1</sup>	Despland <i>et al.</i> , 2011
<b>Acid and brine treated bauxite residue (Bauxsol™**)</b>	Batch adsorption experiment	Kinetics and isotherms	Synthetic water	200 mg P L <sup>-1</sup>	55.72 mg P g <sup>-1</sup>	Ye <i>et al.</i> , 2014
<b>Heat treated bauxite residue</b>	Batch adsorption experiment	Time, pH and initial concentration	Synthetic water	155 mg P L <sup>-1</sup>	155.2 mg P g <sup>-1</sup>	Liu <i>et al.</i> , 2007
<b>Acid and heat treated bauxite residue</b>	Batch adsorption experiment	Time, pH and initial concentration	Synthetic water	155 mg P L <sup>-1</sup>	202.9 mg P g <sup>-1</sup>	Liu <i>et al.</i> , 2007
<b>Acid treated bauxite residue</b>	Batch adsorption experiment	Acid type, pH	Synthetic water	1 mg P L <sup>-1</sup>	1.1 mg P g <sup>-1</sup>	Huang <i>et al.</i> , 2008

822  
823  
824  
825

\*P<sub>max</sub> value given i.e. Maximum amount of P adsorbed per g of media, as determined using the Langmuir adsorption isotherm.

\*\*Bauxsol™ = neutralised bauxite residue produced using the Basecon™ procedure, which uses brines high in Ca<sup>2+</sup> and Mg<sup>2+</sup> (McConchie *et al.*, 2001).

826 **Table 2** Main mineralogical composition (%) of the bauxite residue determined by XRF.

Mineral oxide	%
Aluminum oxide, Al <sub>2</sub> O <sub>3</sub>	14.8 ± 1.5
Iron oxide, Fe <sub>2</sub> O	47.5 ± 2.0
Titanium oxide, TiO <sub>2</sub>	10.3 ± 0.95
Silicon oxide, SiO <sub>2</sub>	7.20 ± 1.0
Calcium oxide, CaO	6.1 ± 1.0

827

828

829

830

831

832

833

834

835

836

837

838

839

840

841

842

843

844

845

846

847 **Table 3** Particle size distribution of the bauxite residue used in this study.

$d_{10}$ ( $\mu\text{m}$ ) <sup>a</sup>	$d_{50}$ ( $\mu\text{m}$ ) <sup>b</sup>	$d_{90}$ ( $\mu\text{m}$ ) <sup>c</sup>
$0.8 \pm 0.1$	$2.6 \pm 0.1$	$6.8 \pm 0.2$

848 <sup>a</sup> $d_{10}$  ( $\mu\text{m}$ ) = the size of particles at 10% of the total particle distribution.

849 <sup>b</sup> $d_{50}$  ( $\mu\text{m}$ ) = the median; the size of particles at 50% of the total particle distribution.

850 <sup>c</sup> $d_{90}$  ( $\mu\text{m}$ ) = the size of particles at 90% of the total particle distribution.

851

852

853

854

855

856

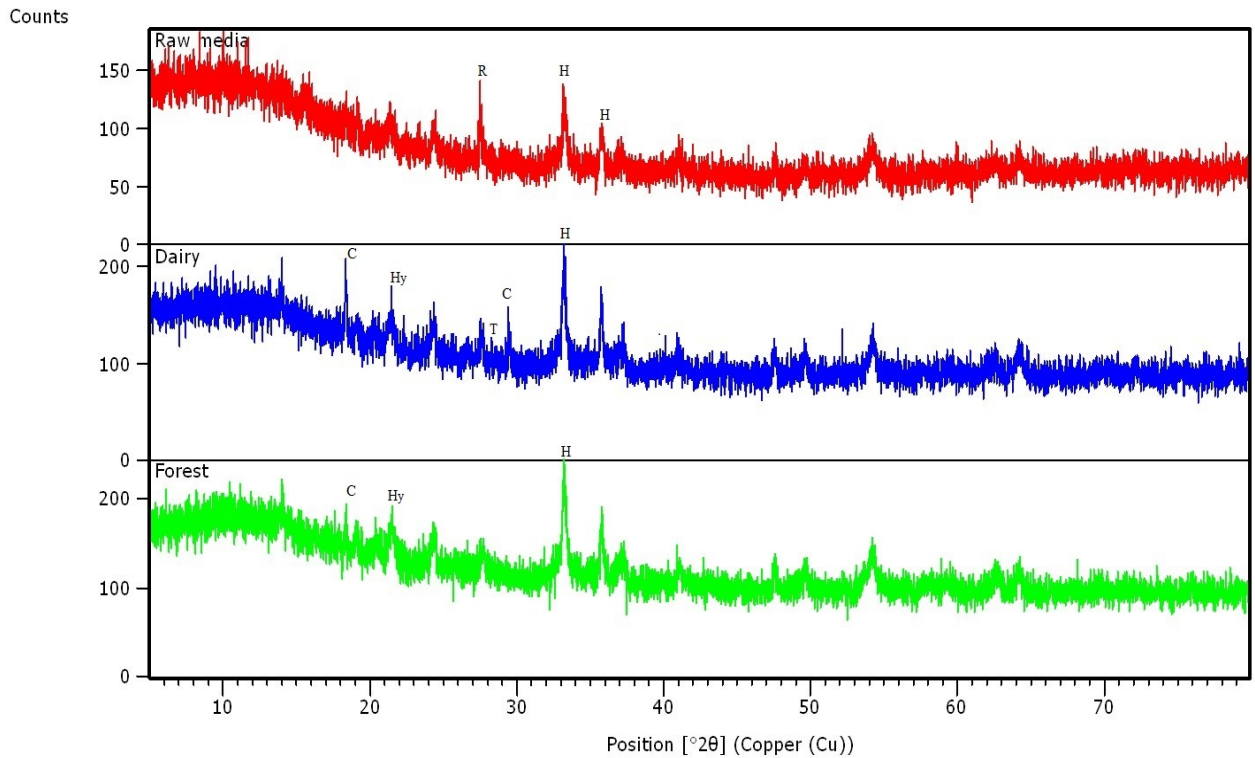
857

858

859

860

861



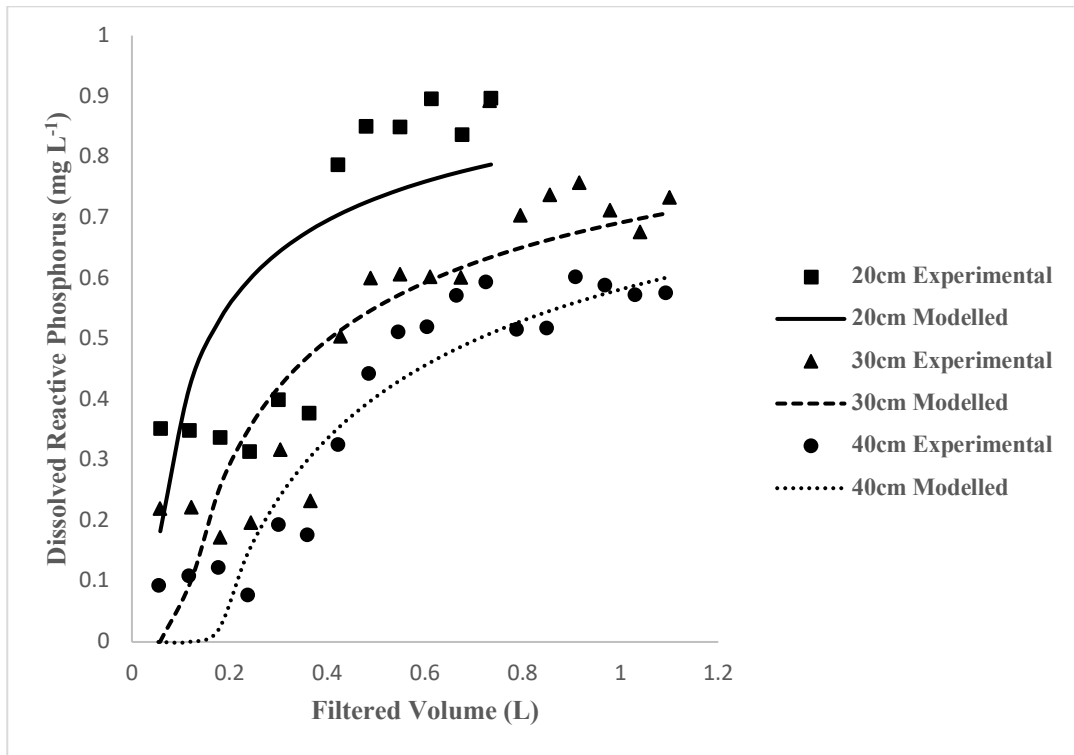
862 **Figure 1** XRD pattern as determined for the column media before ('Raw media', top) and after the  
 863 loading period with DSW ('Dairy', middle) and forest run-off ('Forest', bottom). Hematite (H;  
 864  $\text{Fe}_2\text{O}_3$ ), detected at position 33.153 and 35.612 $^\circ 2\theta$  and rutile (R;  $\text{TiO}_2$ ), detected at position 27.459  
 865  $^\circ 2\theta$  were present in the raw bauxite residue media. Calcium hydrogenphosphate (III) hydrate (C;  
 866  $\text{CaHPO}_4 \cdot 3\text{H}_2\text{O}$ ), detected at positions 19.120 and 30.001  $^\circ 2\theta$ , was present in both the spent media  
 867 following treatment of the DSW and forest run-off.

868

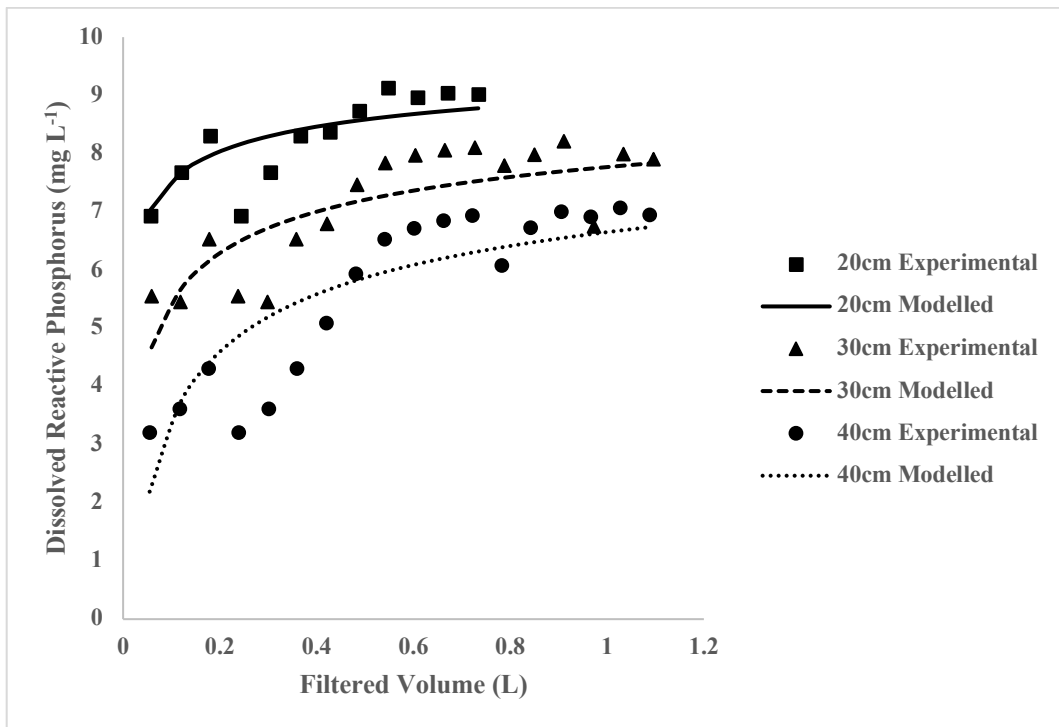
869

870

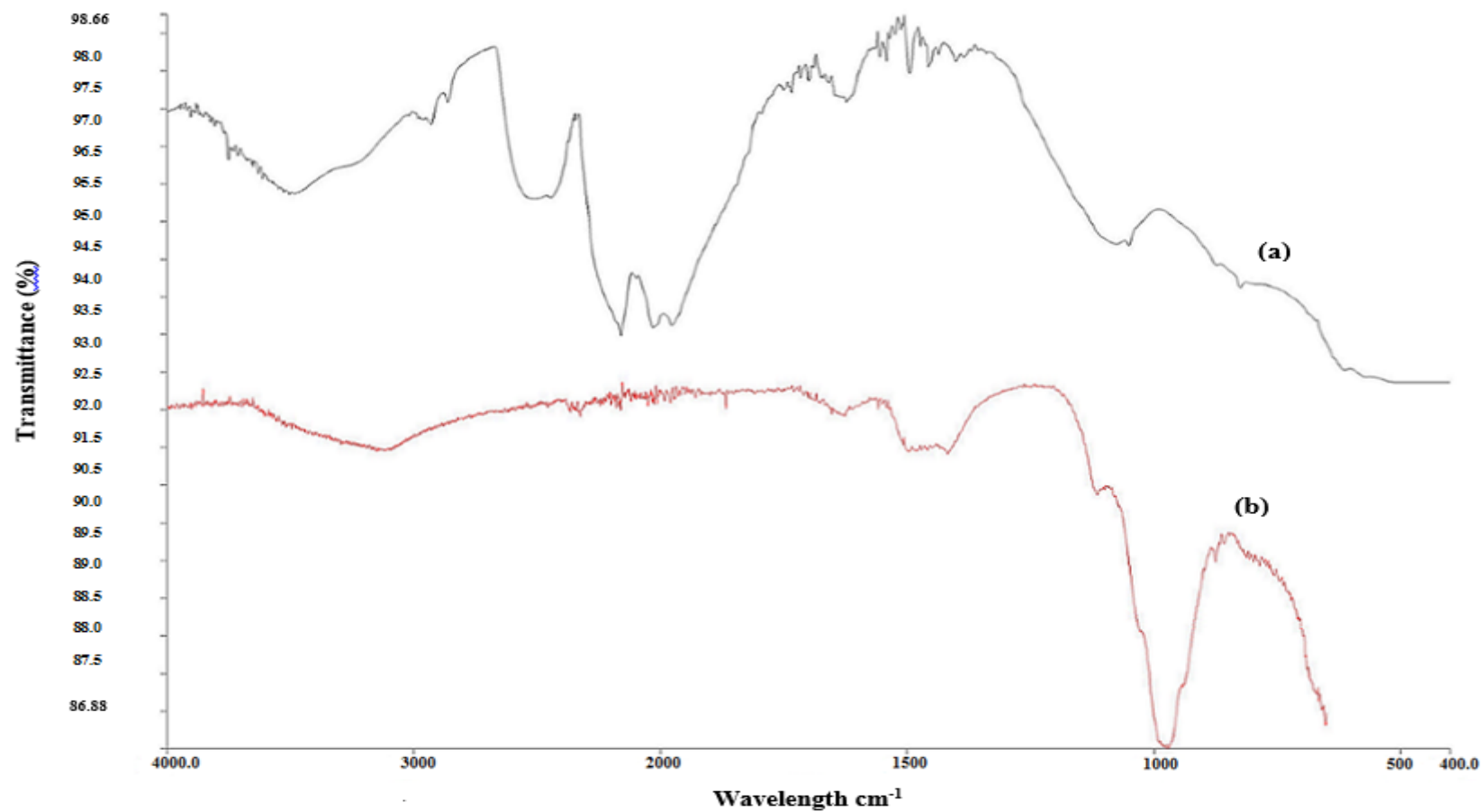
871



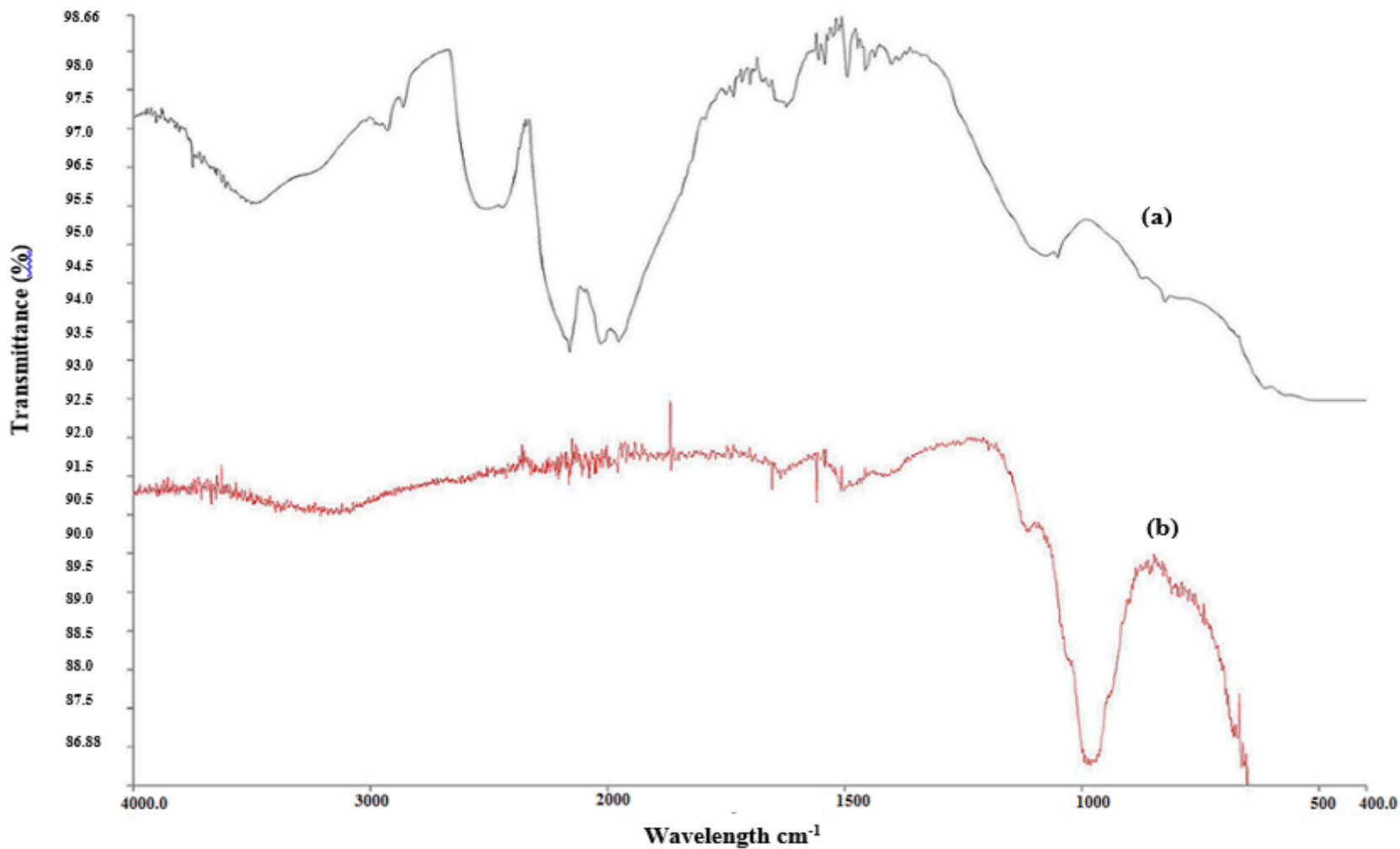
872



873 **Figure 2** The breakthrough curves for the effluent dissolved reactive phosphorus concentration versus  
 874 loading time for forest run-off (top) and dairy soiled water (bottom) using experimental and modelled  
 875 data.

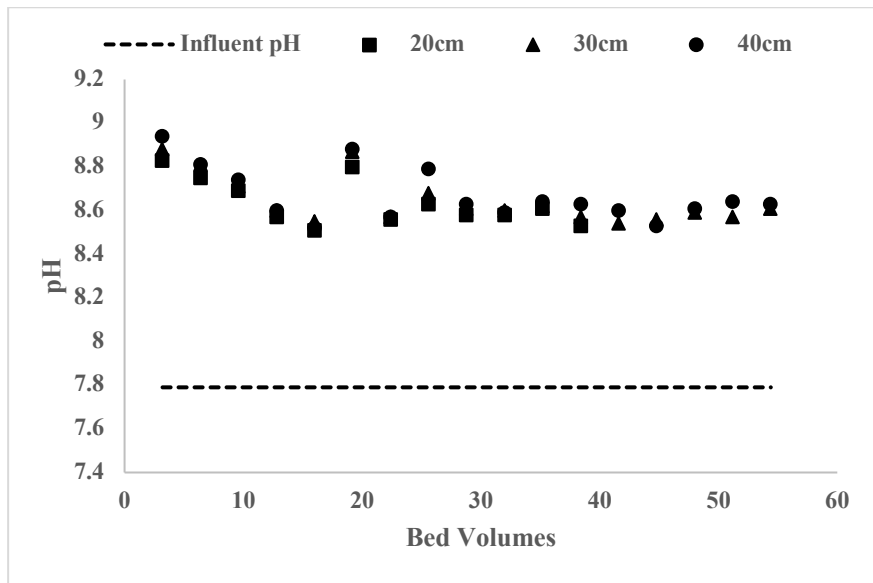


876 **Figure 3** FT-IR analysis of the bauxite residue media before (a) and after use in the column treating DSW (b).

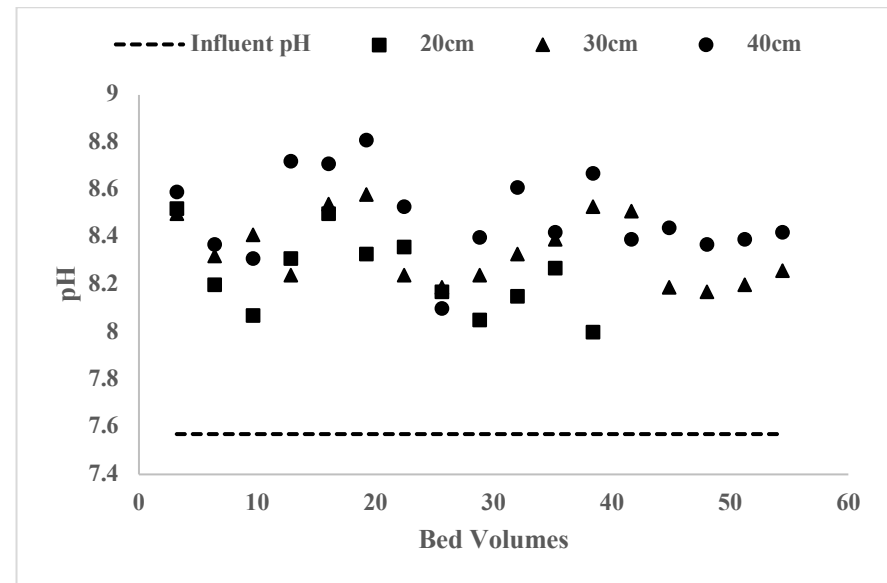


877

**Figure 4** FT-IR analysis of the bauxite residue media before (a) and after use in the column treating forest run-off (b).



(a)



(b)

878 **Figure 5** The pH values of (a) the dairy soiled water and (b) forest run-off effluent from the columns over the 24 – 36 hr loading period, showing that there  
 879 was an overall increase in the pH of the effluent treated.

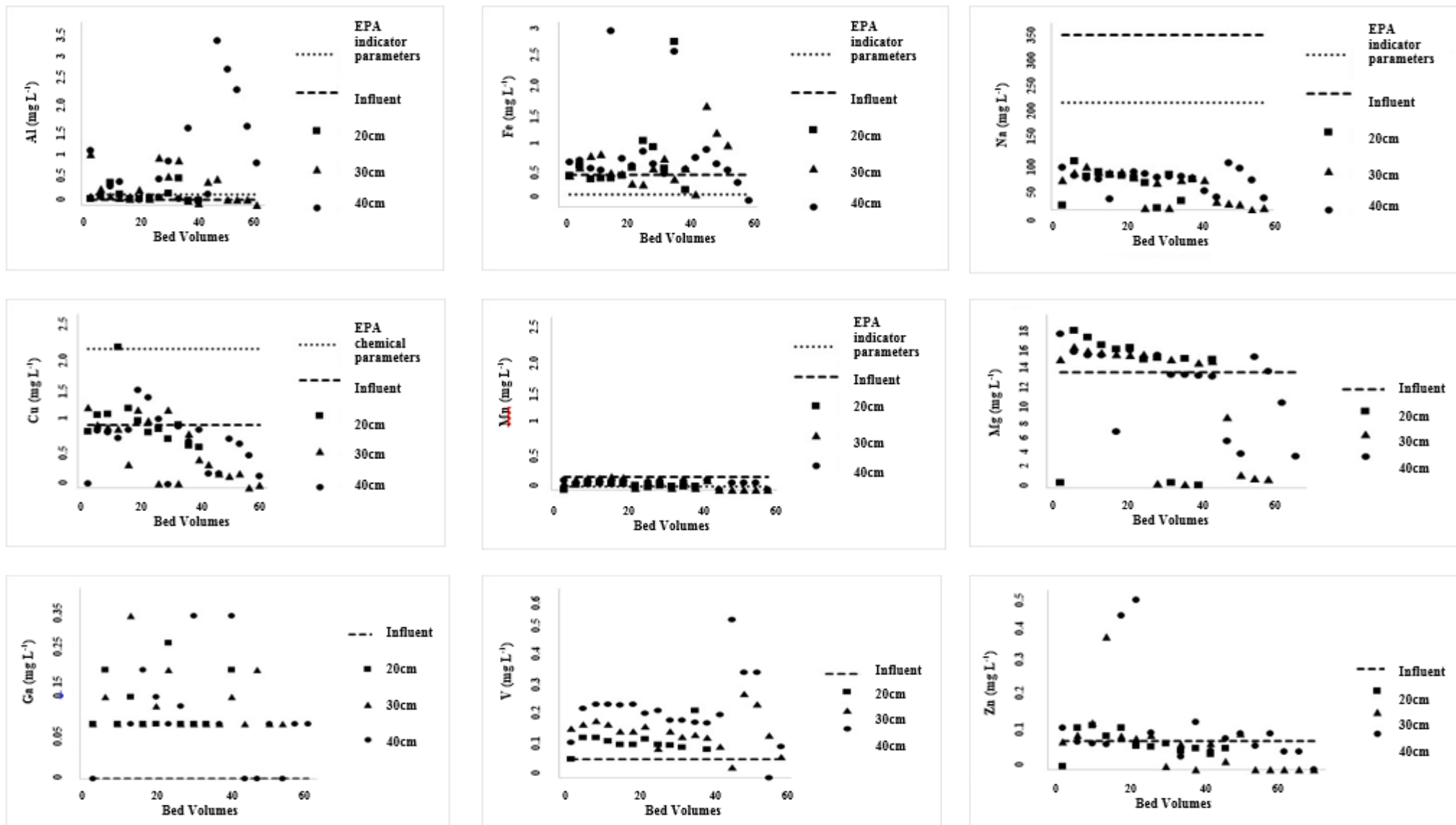
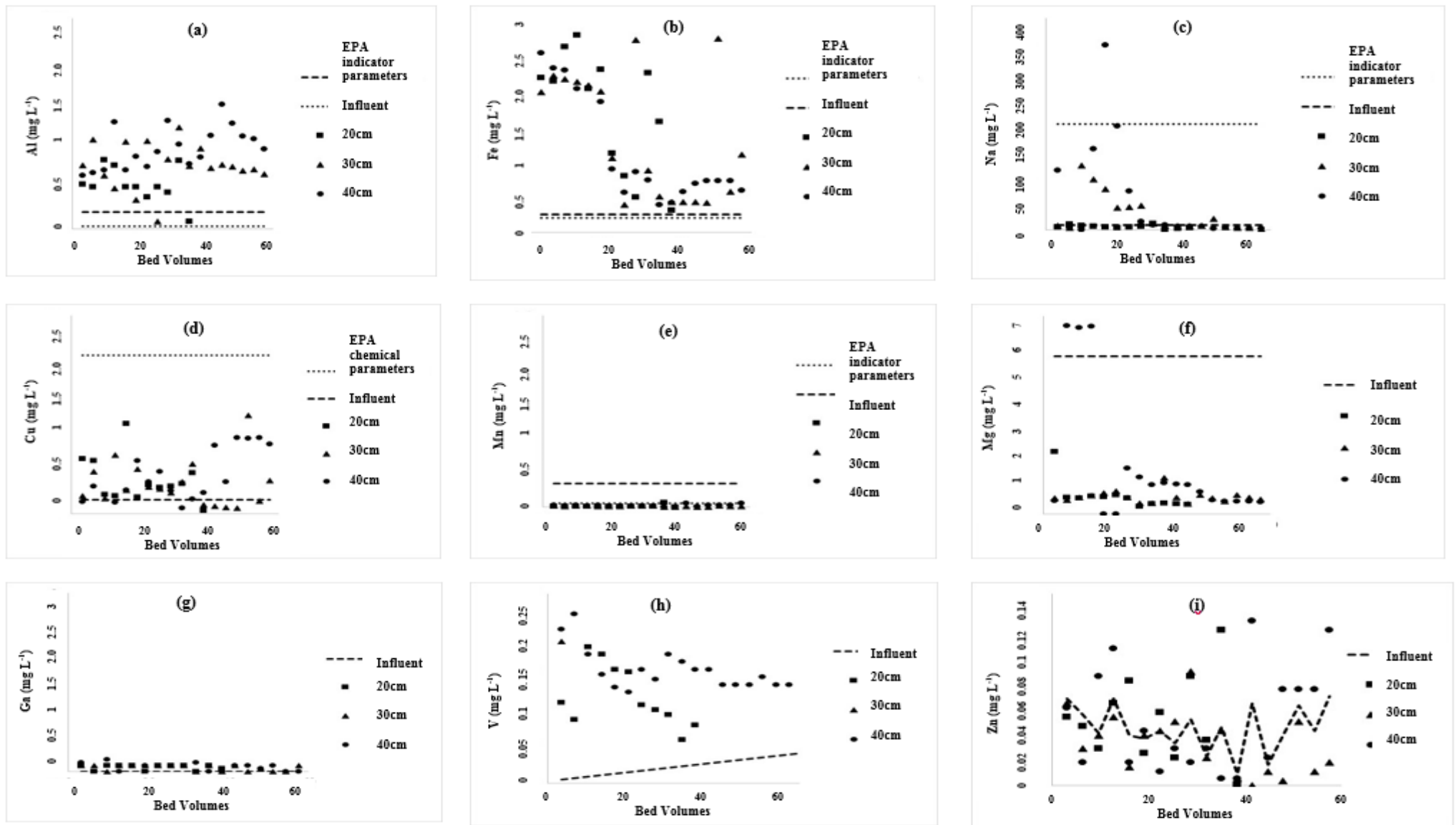


Figure 6 Comparison of the composition of (a) Al, (b) Fe, (c) Na (d) Cu (e) Mn (f) Mg (g) Ga (h) V and (i) Zn in both the influent and effluent in the columns treating DSW over the 24 -36 hr loading period. EPA indicator parameter or EPA chemical parameter included for each element.



3  
4  
5

**Figure 7** Comparison of the composition of (a) Al, (b) Fe, (c) Na (d) Cu (e) Mn (f) Mg (g) Ga (h) V and (i) Zn in both the influent and effluent in the columns treating forest run-off over the 24 -36 hr loading period. EPA indicator parameter or EPA chemical parameter included for each element.

